# Protective role of brain water channel AQP4 in murine cerebral malaria

Dominique Promeneur[a,1], Lisa Kristina Lunde[b], Mahmood Amiry-Moghaddam[b], and Peter Agre[a,1]

[a]Johns Hopkins Malaria Research Institute, Department of Molecular Microbiology and Immunology, Bloomberg School of Public Health, Johns Hopkins University, Baltimore, MD 21205; and [b]Laboratory of Molecular Neuroscience, Centre for Molecular Biology and Neuroscience, Department of Anatomy, University of Oslo, 0317 Oslo, Norway

Contributed by Peter Agre, December 3, 2012 (sent for review September 4, 2012)

**Tragically common among children in sub-Saharan Africa, cerebral malaria is characterized by rapid progression to coma and death. In this study, we used a model of cerebral malaria appearing in C57BL/6 WT mice after infection with the rodent malaria parasite *Plasmodium berghei* ANKA. Expression and cellular localization of the brain water channel aquaporin-4 (AQP4) was investigated during the neurological syndrome. Semiquantitative real-time PCR comparing uninfected and infected mice showed a reduction of brain AQP4 transcript in cerebral malaria, and immunoblots revealed reduction of brain AQP4 protein. Reduction of brain AQP4 protein was confirmed in cerebral malaria by quantitative immunogold EM; however, polarized distribution of AQP4 at the perivascular and subpial astrocyte membranes was not altered. To further examine the role of AQP4 in cerebral malaria, WT mice and littermates genetically deficient in AQP4 were infected with *P. berghei*. Upon development of cerebral malaria, WT and AQP4-null mice exhibited similar increases in width of perivascular astroglial endfeet in brain. Nevertheless, the AQP4-null mice exhibited more severe signs of cerebral malaria with greater brain edema, although disruption of the blood–brain barrier was similar in both groups. In longitudinal studies, cerebral malaria appeared nearly 1 d earlier in the AQP4-null mice, and reduced survival was noted when chloroquine rescue was attempted. We conclude that the water channel AQP4 confers partial protection against cerebral malaria.**

Cerebral malaria is a dangerous complication of infection with *Plasmodium falciparum*, especially in children of sub-Saharan Africa, with a mortality rate of 20% (1). If untreated, cerebral malaria often causes coma and death within 24 h (2). Survivors of cerebral malaria often suffer neurological sequelae such as ataxia, hemiplegia, epilepsy, and blindness. The exact pathogenesis of cerebral malaria remains unclear. It is thought that massive sequestration of erythrocytes containing mature stages of *P. falciparum* within the brain microvasculature (3), as well as an excessive response of the host immune system against the malaria parasite, contribute to the disease (4).

Brain edema and intracranial hypertension are common in cerebral malaria. Elevated cerebrospinal fluid pressure has been reported in more than 80% of African children with cerebral malaria (5, 6). Computed tomography of Kenyan children with cerebral malaria revealed that more than 40% had brain edema (7). More recently, increased brain volume in Malawian children with cerebral malaria based on MRI was reported (8). Severe intracranial hypertension in children with cerebral malaria is often fatal (7, 9). Autopsies of African children who died from cerebral malaria revealed brain edema (10, 11).

A murine model of cerebral malaria has been established in a susceptible strain of mice (C57BL/6) infected with the rodent malaria parasite *P. berghei* ANKA (12). Although relevance to human cerebral malaria in adults has been questioned (13), this model is still considered critical to study underlying mechanisms of cerebral malaria in children (14–16). In this mouse model, monocytes are sequestered in the brain microvasculature, whereas parasitized red blood cells are seen in the human disease. Despite this discrepancy, human cerebral malaria and the experimental murine model of cerebral malaria both include seizures, petechial hemorrhages, and coma followed by death (12, 14, 17) with brain edema (12, 18). MRI of cerebral malaria in mice revealed massive brain edema compressing cerebral arteries, causing coma and death (19).

Abundant in brain, the aquaporin-4 (AQP4) water channel plays multiple roles regulating brain water homeostasis, astrocyte migration, neuronal excitability, and neuroinflammation (20). AQP4 is highly expressed in ependymal cells and astrocytes with polarized distribution in end-feet membranes facing cerebral capillaries and pia mater (21). The strategic location at the blood–brain interface and the cerebrospinal fluid–brain interface makes AQP4 a major factor in regulation of water movement into and out of the brain. AQP4 has been investigated in brain edema associated with multiple forms of brain injury such as stroke, meningitis, neuromyelitis optica, and brain tumor (22). A role for AQP4 in cerebral malaria has recently been suggested by light microscopy (23, 24). To clarify participation of AQP4 in the pathophysiology of cerebral malaria, we analyzed AQP4 mRNA and protein expression and performed immunoelectron microscopy of brain in control and AQP4-null mice. Our studies support a protective role for AQP4 in murine cerebral malaria. Therapeutic treatments based on AQP4 when available may improve clinical outcome in cerebral malaria.

## Results

A well-established experimental mouse model of cerebral malaria was used (12, 18). C57BL/6 WT mice infected with *P. berghei* ANKA developed cerebral malaria with increased brain water content (Fig. 1*A*). Existence of cerebral malaria was confirmed by analysis of marker proteins. Increased expression of the intercellular adhesion molecule 1 (ICAM-1) on activated brain endothelial cells was detected by immunoblot (Fig. 1*B*). Increased expression of the astrocyte-specific marker GFAP was assessed by immunofluorescence microscopy (Fig. 1*C*). Such increased expressions of ICAM-1 and GFAP are known to occur in murine cerebral malaria (25, 26).

To examine whether the astrocyte water channel AQP4 was affected during cerebral malaria, C57BL/6 WT mice were infected with *P. berghei* ANKA and expression of AQP4 was investigated. Semiquantitative real-time PCR revealed a strong decrease in AQP4 mRNA expression in cerebral malaria ($0.28 \pm 0.02\%$ vs. $0.65 \pm 0.09\%$; $P < 0.05$; $n = 5$–7; Fig. 2*A*). Immunoblots of whole brain samples revealed partially decreased expression of AQP4 protein in mice with cerebral malaria ($81.1 \pm 4.3\%$) compared with control levels ($100 \pm 3.5\%$; $P < 0.05$; $n = 5$; Fig. 2 *B* and *C*). Anti-AQP4 immunogold EM was used to assess the distribution and level of expression of AQP4 protein in brains of mice with cerebral malaria. EM revealed membrane polarization of AQP4 at the perivascular astrocyte processes and end-feet swelling in the mice

Author contributions: D.P. and P.A. designed research; D.P., L.K.L., and M.A.-M. performed research; D.P., L.K.L., M.A.-M., and P.A. analyzed data; and D.P., M.A.-M., and P.A. wrote the paper.

The authors declare no conflict of interest.

[1]To whom correspondence may be addressed. E-mail: dpromene@jhsph.edu or pagre@jhsph.edu.

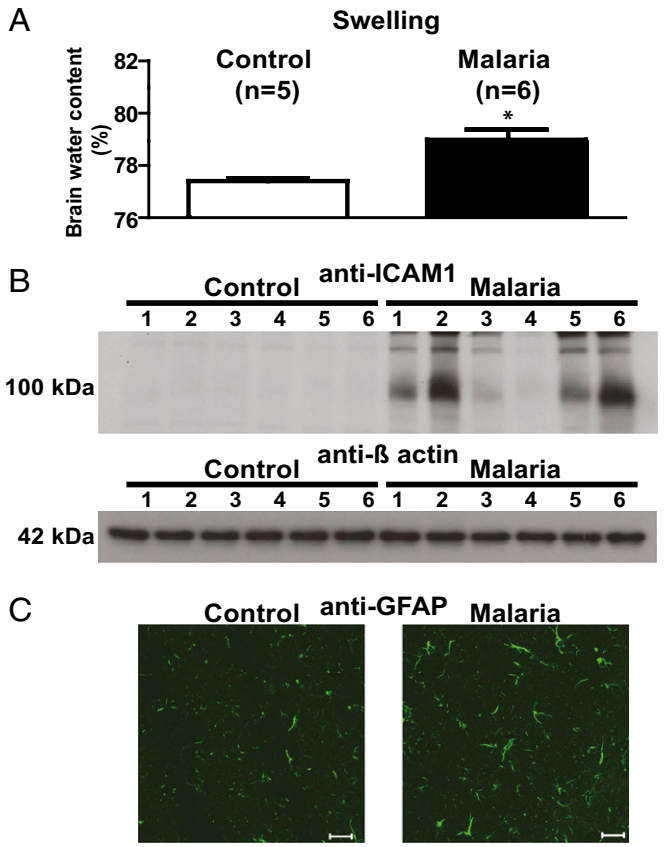


**Fig. 1.** Brain edema in murine cerebral malaria. Uninfected C57BL/6 control mice and littermates infected with $10^6$ *P. berghei* parasites were evaluated 7 to 8 d postinfection when signs of experimental cerebral malaria appeared. (*A*) Brain water content, assessed from the wet-to-dry-weight ratio, was 2.07% higher in mice with cerebral malaria than in uninfected controls. Values are mean ± SEM (*$P \leq 0.05$, Student *t* test.) (*B*) Representative immunoblot shows induction of ICAM-1 expression in brains of mice with cerebral malaria. (*C*) Representative immunofluorescence microscopy shows increased expression of GFAP in brains of mice with cerebral malaria. (Scale bar: 20 μm.)

with cerebral malaria (Fig. 3 *A* and *B*). Quantification of AQP4 expression confirmed a partial reduction of AQP4 at the perivascular and the subpial membranes of astroglia in mice with cerebral malaria (Fig. 4). Linear density of anti-AQP4 immunogold particles per micrometer was lower in mice with cerebral malaria than in control mice at perivascular membranes (2.59 ± 1.25 vs. 3.04 ± 1.14; $P < 0.05$; $n = 4$) and subpial membranes (2.97 ± 1.09 vs. 3.97 ± 1.36; $P < 0.01$; $n = 4$).

To further investigate the role of AQP4 protein in cerebral malaria, AQP4-null mice with C57BL/6 genetic background were infected with *P. berghei* ANKA. EM analysis performed at the apparent onset of cerebral malaria showed that AQP4-null mice also developed an increase in width of perivascular astrocyte endfeet (Fig. 5 *A* and *B*). When EM images of WT and AQP4-null brains were directly compared, end-feet widths were similar in brains of uninfected mice but increased comparably with appearance of cerebral malaria (Fig. 6). At the outset of the experiment, WT and AQP4-null mice appeared similar, but cerebral malaria appeared earlier in the AQP4-null mice. Most WT mice still appeared normal at the beginning of day 6 postinfection, whereas some AQP4-null mice were already showing signs of cerebral malaria, such as reduced mobility, ruffled coat, hunched back, or coma. Neurological impairment was scored according to the grading system of Waknine-Grinberg et al. (27) in which greater disease severity is associated with higher scores. Body weight and temperature scores were similar for AQP4-null and WT mice; however AQP4-null mice exhibited higher clinical scores for abnormal appearance and behavior compared with WT mice (Fig. 7).

Examination of brains of mice with cerebral malaria yielded a subtle difference. The AQP4-null mice with cerebral malaria consistently displayed greater brain water content than their infected WT littermates (80.10 ± 0.75% vs. 77.71 ± 0.11%; $P < 0.05$; $n = 5$; Fig. 8*A*). Despite abnormalities in brain water homeostasis, the integrity of the blood–brain barrier, as assessed by leakage of Evans blue dye from the vascular space, was disrupted similarly in WT and AQP4-null mice (Fig. 8*B*). The effect of AQP4 deficiency on survival from cerebral malaria was analyzed by Kaplan–Meier plot. WT and AQP4-null mice all survived the first 5 d postinfection, but some of each group became sick and began to die on the sixth day (Fig. 9*A*). By the end of day 6, survival of AQP4-null mice was reduced compared with WT littermates (31.6 ± 7.54% vs. 85.7 ± 5.91%). Survival was further reduced in both groups by the end of day 8 (5.26 ± 3.62% vs. 14.3 ± 5.91%). All mice were dead after the 10th day postinfection. These survival differences were of statistical significance ($P < 0.001$; $n = 35$ AQP4-null mice and $n = 37$ WT mice). To confirm a potentially protective role for AQP4 in cerebral malaria, a rescue experiment was undertaken. Chloroquine was administrated twice daily to all mice beginning on the morning of day 6 (Fig. 9*B*). By this time, the AQP4-null mice were already showing more pronounced signs of illness. Chloroquine treatment was continued until day 15, by which time only 20% of AQP4-null mice survived, whereas 70% of WT mice were still alive ($P < 0.05$; $n = 10$).

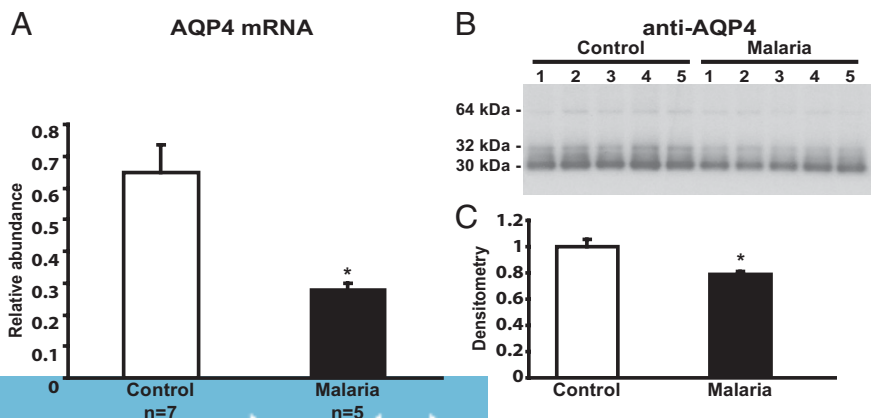


**Fig. 2.** Reduced brain AQP4 mRNA and protein in murine cerebral malaria. Uninfected control mice and littermates with cerebral malaria were killed 7 to 8 d postinfection. (*A*) Semiquantitative real-time PCR of AQP4 mRNA in cerebral malaria. Analysis showed that brain AQP4 mRNA was reduced by 57% in murine cerebral malaria. Values are mean ± SD. (*B*) Anti-AQP4 immunoblot of brain membranes revealed 32 to 34 kDa AQP4 splice variants and 64 kDa AQP4 dimers. (*C*) Densitometric analysis showed brain AQP4 protein was decreased by 20% in murine cerebral malaria. Values are mean ± SEM (*$P \leq 0.05$, Student *t* test). Data are representative of three independent experiments.

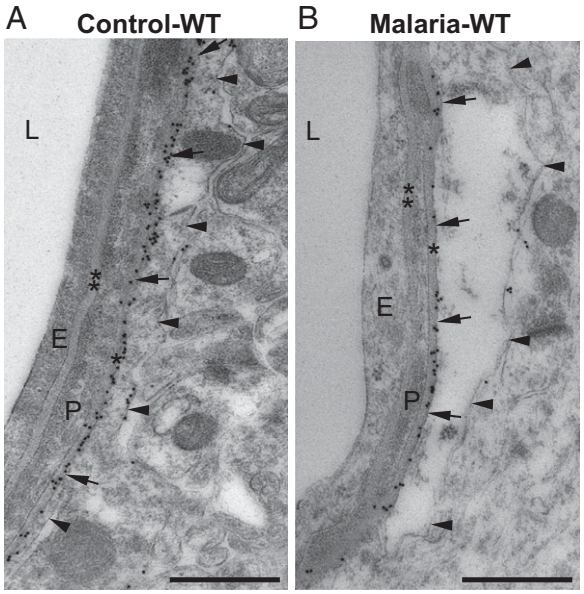


**Fig. 3.** Anti-AQP4 immunogold EM of murine cerebral malaria. (*A* and *B*) Ultrathin Lowicryl sections of perfused fixed brains from uninfected control mice or mice with cerebral malaria killed 7 to 8 d postinfection. Anti-AQP4 immunogold labeling of astrocyte perivascular end-feet in membranes facing endothelial basal lamina (arrows) or membranes facing neuropil (arrowheads). Single asterisk marks basal lamina between the pericyte and astrocyte end-foot; double asterisk marks basal lamina between the endothelial cell and pericyte. E, endothelial cell; L, capillary lumen; P, pericyte. (Scale bar: 500 nm.)

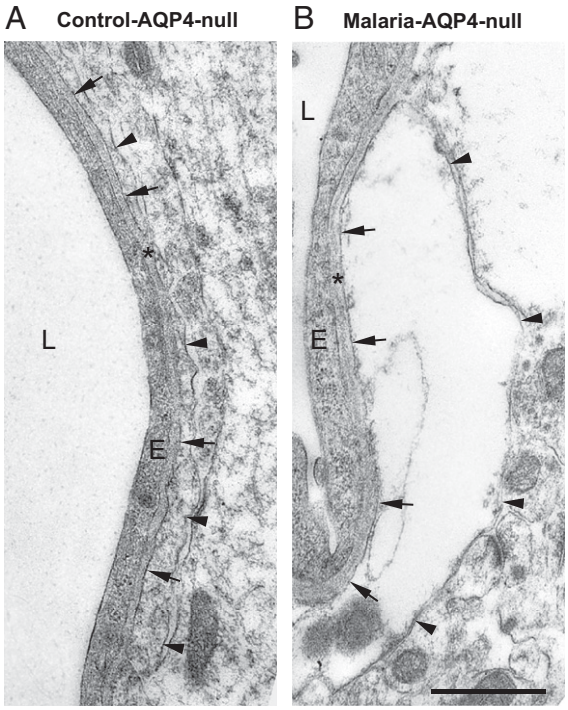


**Fig. 5.** EM image of AQP4-null brain in murine cerebral malaria. (*A* and *B*) Ultrathin Lowicryl sections of brains from uninfected AQP4-null mice or AQP4-null mice with cerebral malaria killed 6 d postinfection. The sections were incubated together with the WT sections shown in Fig. 3. As expected, no AQP4 immunogold labeling is observed in the AQP4-null mice. Astrocyte end-feet are identified in membranes facing endothelial basal lamina (arrows) or membranes facing neuropil (arrowheads). Asterisk indicates basal lamina between the endothelium and astrocyte endfoot. E, endothelial cell; L, capillary lumen. (Scale bar: 500 nm.)

## Discussion

Aquaporin water channels facilitate rapid transmembrane movements of water into and out of cells (28). Found in all forms of life, aquaporins are involved in multiple physiological and pathophysiological pathways (29). The fourth member of the aquaporin water channel family, AQP4, bears several distinctive features (30, 31). AQP4 is resistant to mercurial inhibition because of the absence of a specific cysteine residue within the pore. AQP4 exists as two isoforms as a result of alternative translation initiation at M1 or M23 (32-33). M23 preferentially forms large square arrays as a result of self-assembly (34).

AQP4 has attracted large attention as a result of its preponderance within the central nervous system (reviewed in ref. 35). Abundant at brain–liquid interfaces, AQP4 regulates water exchange between blood or cerebrospinal fluid and brain parenchyma. AQP4 is highly enriched in membranes of astrocyte end-feet processes surrounding vascular endothelium, beneath ependymal cells that line the ventricles, and beneath pia mater at the brain surface. In contrast, AQP4 density is much lower at the astrocyte membrane domains facing the neuropil (21, 36). The markedly polarized distribution of AQP4 involves a PDZ binding domain at the C terminus of AQP4 that is linked to α-syntrophin, a member of the dystrophin-associated proteins (37).

AQP4 has been studied in mouse models of multiple brain disorders (reviewed in refs. 22, 38). AQP4-null mice are partially protected from brain edema caused by hyponatremia or ischemia

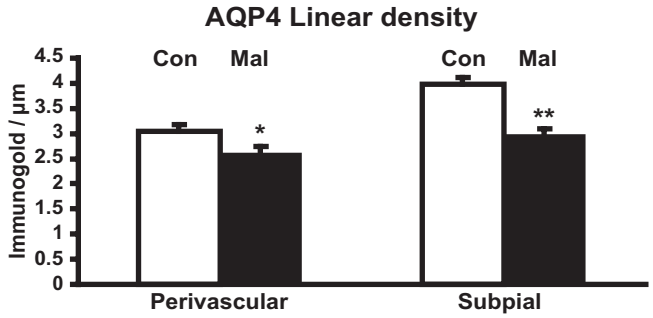


**Fig. 4.** Quantification of AQP4 immunolabeling in uninfected control mice (open bars) and mice with cerebral malaria 7 to 8 d postinfection (closed bars). The values along the ordinate represent the number of immunogold particles per micrometer in the perivascular (*Left*) and subpial (*Right*) membrane domains of the astroglial end-feet. Values are mean ± SE (*$P \leq 0.05$, **$P \leq 0.01$, Student *t* test).

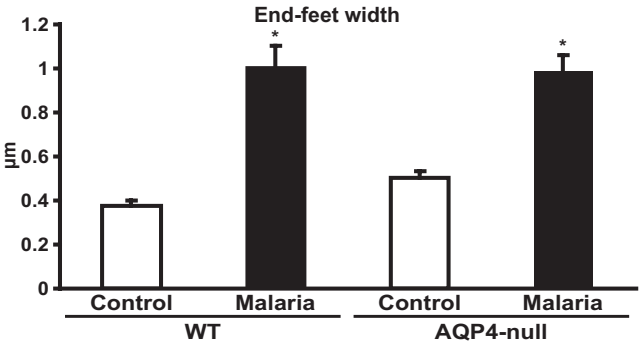


**Fig. 6.** Quantification of astrocyte end-feet width in WT and AQP4-null mice without (open bars) and with cerebral malaria 6 d postinfection (closed bars). Values are mean ± SE (*$P \leq 0.01$, ANOVA).

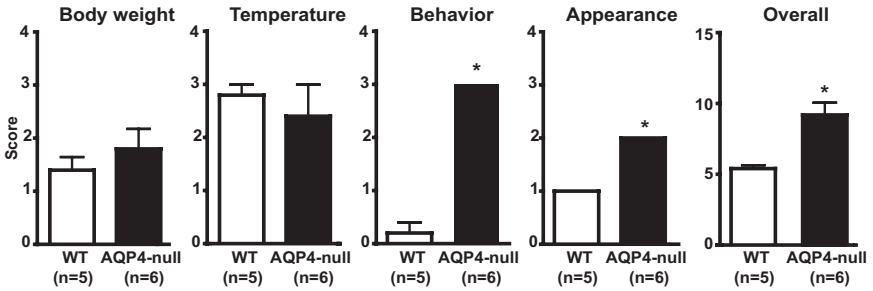


**Fig. 7.** Severity of cerebral malaria in AQP4-null mice. WT and AQP4-null mice were infected with $10^6$ *P. berghei* parasites and their clinical scores compared on day 6 postinfection. Loss of body weight, reduced body temperature, appearance, and behavior were graded. Greater disease severity is associated with higher scores. AQP4-null mice exhibited higher clinical scores for appearance and behavior and overall clinical scores compared with WT mice. Values are mean ± SEM (*$P \leq 0.05$, Student *t* test). Data are representative of four independent experiments.

(39). AQP4 mislocalization partially protects against reperfusion injury after transient middle cerebral artery occlusion in α-syntrophin–null mice (40). AQP4 deficiency in mice appears to worsen the outcome from brain tumor, abscess, cortical freezing, and subarachnoid hemorrhage (41, 42). Thus, deficiency or mislocalization of AQP4 protect against cytotoxic (cellular) brain edema with intact blood–brain barrier, whereas AQP4 facilitates clearance of vasogenic (leaky vessel) edema with defective blood–brain barrier.

Evidence linking AQP4 to other neural disorders is emerging. Deficient or mislocalized AQP4 increased susceptibility to epileptic seizures and exacerbated the severity (43, 44). Deficiency of AQP4 was noted in epileptogenic locus in hippocampus from some humans with mesial temporal lobe epilepsy (45). AQP4 has been implicated in astrocyte migration and may delay glial scarring during wound healing (46). AQP4 is specifically involved in neuromyelitis optica, a recurrent demyelinating disease of optic nerve and spinal cord causing blindness and paralysis (reviewed in ref. 47). Cerebral presentations are far more common in children than in adults (48). Circulating autoantibodies to astroglial membranes had been identified in the majority of patients with neuromyelitis optica, but not in patients with multiple sclerosis, a common demyelinating disease with which neuromyelitis optica was sometimes confused (49). Autoantibodies from patients with neuromyelitis optica react specifically with external domains of AQP4 (50) and explain clinical variability (51).

Cerebral malaria has enormous clinical importance for children in sub-Saharan Africa (4). A mouse model of cerebral malaria exists (12). C57BL/6 mice infected with the rodent malaria parasite *P. berghei* ANKA reproducibly manifest cerebral malaria at 1 wk postinfection. Similar to cerebral malaria in human children, sensitive strains of mice rapidly decline into coma, with cerebral edema and hypertension (19). In contrast, adult humans with cerebral malaria exhibit a different course, with evidence indicating that inflammation and edema are less critical in older patients (13).

AQP4 water channels have recently been studied in cerebral malaria. Comparing a cerebral malaria-susceptible strain of mice vs. a resistant strain by light microscopy, greater expression of brain AQP4 was documented in the susceptible mice (24). This caused the investigators to consider AQP4 as a factor contributing to the deleterious consequences of cerebral malaria, and an AQP4

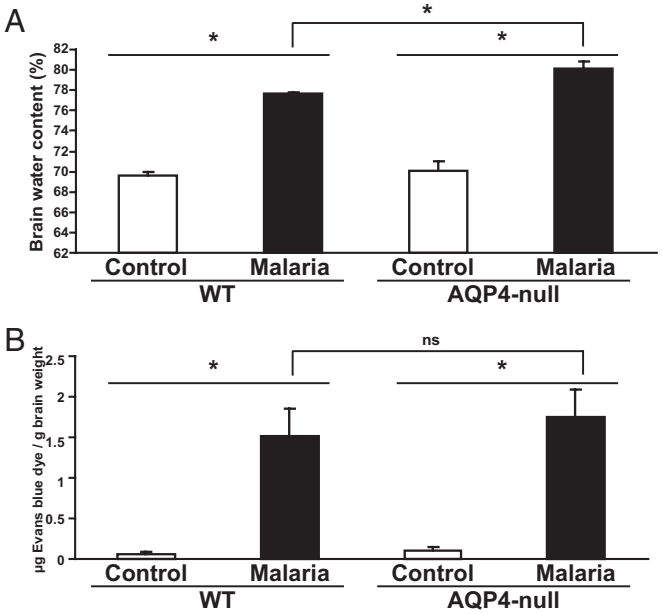


**Fig. 8.** Brain edema in AQP4-null mice with cerebral malaria. WT and AQP4-null mice were infected with $10^6$ *P. berghei* parasites and evaluated on day 6 postinfection. (*A*) Brain water content was similar in WT and AQP4-null mice in basal conditions and increased during cerebral malaria with greater increase in the AQP4-null mice compared with WT mice. (*B*) Blood–brain barrier disruption assessed by Evans blue dye leakage from the brain microvasculature was similar in both groups during cerebral malaria. Values are mean ± SEM for each group and are representative of three independent experiments (*$P \leq 0.05$, Student *t* test).

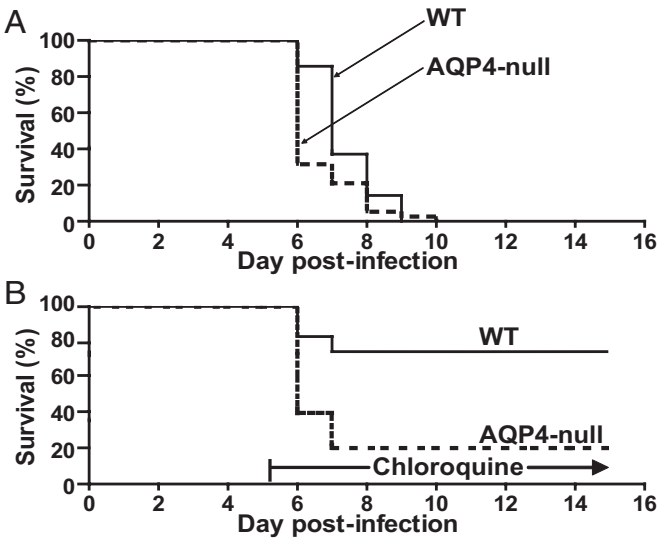


**Fig. 9.** Accelerated mortality from cerebral malaria in AQP4-null mice. WT and AQP4-null mice infected with $10^6$ *P. berghei* parasites were monitored for survival. (*A*) Earlier deaths were seen in the AQP4-null mice compared with WT mice during the progression of cerebral malaria. Survival data are pooled from four independent experiments ($P \leq 0.01$; $n = 35$ WT mice; $n = 37$ AQP4-null mice). (*B*) Chloroquine was administered to mice twice per day beginning on the morning of day 6. By day 15, only 20% of AQP4-null mice were rescued from cerebral malaria vs. 70% of the WT mice. Data are survival probabilities and SEs as determined by Kaplan–Meier analysis ($P \leq 0.05$; $n = 10$ WT mice; $n = 10$ AQP4-null mice).

threshold was proposed above which infected mice can no longer compensate. It was suggested that AQP4 might be a target for therapeutic intervention to prevent cerebral malaria. A second recent light microscopy study of Vietnamese adults who had died of cerebral malaria revealed a modest, statistically insignificant increase of AQP4 in brainstem but not midbrain or cortex (23). The investigators postulated that AQP4 may confer neuropathological and neuroprotective responses to cerebral malaria in adult humans. Both aforementioned studies used immersion fixation of whole brain with light microscope imaging, without resolution to assess subcellular distribution, and neither used mRNA or protein analyses. With different methodologies, our studies reached a different conclusion. Rigorous methods to prevent protein degradation documented a 20% decrease in AQP4 expression in murine cerebral malaria (Fig. 2). The decrease in AQP4 in murine cerebral malaria was confirmed by high-resolution immunocytochemistry of astrocytes at perivascular and subpial locations, but the polarized distribution of AQP4 was not altered in cerebral malaria (Fig. 3). The decrease in AQP4 protein may primarily result from the reduced AQP4 mRNA abundance. It may also result from posttranslational mechanisms, as the AQP4 protein can be endocytosed and trafficked to lysosomal compartment for degradation (52). Potential candidates for the AQP4 decrease may be hypoxia, endothelin-1, or thrombin, all known to be present or increased in cerebral malaria and to reduce AQP4 (53-61).

Analysis of mice with targeted disruption of the gene encoding AQP4 revealed a protective role for AQP4 in cerebral malaria. EM studies of brains from WT mice and AQP4-null mice exhibited similar tissue morphologies (Figs. 3*A* and 5*A*). When afflicted with cerebral malaria, both strains of mice exhibit similar cytotoxic edema as reflected by similar swelling of perivascular end-feet (Figs. 3*B* and 5*B*). Both strains of mice also exhibit similar disruption of the blood–brain barrier in response to malarial infection as assessed by Evans blue dye leakage, which represents evidence of vasogenic edema (Fig. 8). However, multiple measures of clinical status were more severely abnormal in the AQP4-null mice with cerebral malaria (Fig. 7). Brain water content of the AQP4-null mice was higher (Fig. 8). The AQP4-null mice showed accelerated mortality and resistance to chloroquine rescue (Fig. 9). The AQP4-null mice reached the terminal phase of the disease earlier than their WT littermates, and they could no longer be rescued by chloroquine. Taken together, these findings suggest that vasogenic edema predominates in murine cerebral malaria and that the protective effect of AQP4 is via the ensuing vasogenic edema.

In conclusion, our studies support a protective role for AQP4 in cerebral malaria. While AQP4 levels were modestly decreased in cerebral malaria, their distribution was unchanged. Similar to WT littermates, uninfected AQP4-null mice had no obvious abnormalities. Reduced ability to eliminate edema during cerebral malaria is presumed to explain the susceptibility of AQP4-null animals. When the profound evolutionary pressure of malaria is considered, even small advantages in clinical presentation and survival are likely to have significant consequences on populations.

## Materials and Methods

**Mice, Parasites, and Drug Treatment.** AQP4-null mice were generated by targeted gene disruption as described by Thrane at al (62) and backcrossed at least 10 times onto the C57BL/6 genetic background with normal mice (Jackson Laboratory). All experiments used methods and guidelines approved by the Animal Ethical Care Committee of Johns Hopkins University in compliance with US guidelines for the use of animals in research. Eight- to 12-wk-old female mice were infected with *P. berghei* ANKA (PbA MRA-311; Centers for Disease Control and Prevention) by i.p. injection of $10^6$ infected red blood cells. Survival was monitored each day, and parasitemia (percentage of infected red blood cells) was assessed every other day by examination of Giemsa-stained tail blood smears. The disease severity was scored according to a grading system described by Waknine-Grinberg et al. (27). This grading system considers changes in appearance and behavior, the loss of body weight and decrease in body temperature. In some experiments, mice were treated with chloroquine (10 mg/kg body weight; Sigma-Aldrich) dissolved in PBS solution and administered by i.p. injection.

**Antibodies.** We used the following antibodies: AQP4 (catalog no. AB3594; Millipore), an affinity-purified rabbit polyclonal antibody against AQP4; ICAM-1 (catalog no. MAB1397Z; Millipore), a monoclonal antibody against ICAM-1; β-actin (catalog no. A1978; Sigma-Aldrich), a monoclonal antibody against β-actin; and GFAP (catalog no. 10-0300; Invitrogen), an affinity-purified rat polyclonal antibody against GFAP.

**Immunoblotting.** Immunoblotting of whole brains was performed as previously described (63). AQP4 protein level in the experimental animals were calculated as fraction of control levels and normalized to 100%.Values were presented as means ± SEM.

**Preparation of RNA Samples and Semiquantitative Real-Time PCR.** Total RNA was extracted from the cerebrum and reverse-transcribed to cDNA. The quantitative PCR was performed by using SYBR Green real-time PCR Master Mix (Applied Biosystems) according to the manufacturer's instructions. We used the following primers: 5′-GAGTCACCACGGTTCATGGA-3′ (sense) and 5′-CGTTTGGAATCACAGCTGGC-3′ (antisense) for AQP4 and 5′-TGTATGCCTCTGGTCGTACC-3′ (sense) and 5′-CAGGTCCAGACGCAGGATG-3′ (antisense) for β-actin. Changes in AQP4 and β-actin mRNA values were estimated by raising the reaction efficiency to the exponent power of the negative threshold cycle (E-Ct) (64). AQP4 mRNA values were normalized to those of β-actin used as internal controls. Values were presented as means ± SD.

**Immunogold EM.** Mice were perfused through the heart with 4% formaldehyde in phosphate buffer containing 0.2% picric acid at pH 6.0, then pH 10.0, for quantitative immunogold analysis (40), and with a mixture of 4% formaldehyde and 0.1% glutaraldehyde in phosphate buffer for measurement of end-feet swelling. Brain specimens were embedded in methacrylate resin (Lowicryl HM20). Ultrathin sections were incubated with antibodies to AQP4 followed by goat anti-rabbit antibody coupled to 15-nm colloidal gold and examined by using a CM 10 electron microscope (Philips) (38). For the quantification of AQP4 immunogold labeling, digital images of sections from four malaria infected mice (80 images) and three control mice (81 images) were acquired and quantified with a commercial image analysis program (Soft Imaging Systems). Non–end-feet labeling density was measured as labeling per unit area excluding all perivascular processes. For the quantification of the end-feet swelling, ultrathin sections were contrasted by 0.3% uranyl acetate and 1% lead citrate, and 25 to 30 digital transmission EM images containing astrocytic end-feet adjacent to brain capillaries were randomly acquired from each section. Swelling of end-feet was calculated by dividing end-feet area by length of the membrane facing the basal lamina with the software program ImageJ. Mean value of the groups (WT control, $n$ = 3, 72 end-feet; WT malaria, $n$ = 3, 81 end-feet; AQP4-null control, $n$ = 3, 70 end-feet; AQP4-null malaria, $n$ = 4, 105 end-feet) were compared by ANOVA. Data are presented as mean ± SE.

**Brain Water Content.** After mice were killed, brains were removed, weighed to assess wet weight (WW), dried for 24 h at 80 °C, and weighed to assess dry weight (DW). The brain water content, as a percentage, was calculated by the following formula: [(WW − DW)/WW] × 100.

**Blood–Brain Barrier Disruption.** Mice were injected i.v. with 0.2 mL of 2% Evans blue dye (Sigma-Aldrich) in PBS solution on day 6 after infection. One hour later, mice underwent intracardiac perfusion with PBS solution, and their brains were removed. Brains were weighted and immersed in 2 mL formamide at 37 °C for 48 h. Dye extravasation was measured by optical absorbance at 620 nm and compared with Evans blue/formamide standards. Results are reported as micrograms Evans blue dye per gram of brain tissue.

**Statistical Analysis.** Statistical analyses were assessed by an unpaired $t$ test or ANOVA whereby several groups were analyzed. Data were presented as mean ± SEM. The Kaplan–Meier test was used for analysis of survival curves. Differences in which $P < 0.05$ were considered statistically significant.

**ACKNOWLEDGMENTS.** We thank the Parasitology Core Facility at Johns Hopkins Malaria Research Institute for supplying malarial parasites. This work was supported by the Bloomberg Family Foundation, National Institutes of Health Grants R01HL48268 and U19AI089680 (to P.A.), and a grant from the Research Council of Norway (to M.A.-M.).

1. Jaffar S, Van Hensbroek MB, Palmer A, Schneider G, Greenwood B (1997) Predictors of a fatal outcome following childhood cerebral malaria. *Am J Trop Med Hyg* 57(1): 20–24.
2. Newton CR, Krishna S (1998) Severe falciparum malaria in children: Current understanding of pathophysiology and supportive treatment. *Pharmacol Ther* 79(1): 1–53.
3. Dorovini-Zis K, et al. (2011) The neuropathology of fatal cerebral malaria in Malawian children. *Am J Pathol* 178(5):2146–2158.
4. Idro R, Jenkins NE, Newton CR (2005) Pathogenesis, clinical features, and neurological outcome of cerebral malaria. *Lancet Neurol* 4(12):827–840.
5. Newton CR, et al. (1991) Intracranial pressure in African children with cerebral malaria. *Lancet* 337(8741):573–576.
6. Waller D, et al. (1991) Intracranial pressure in childhood cerebral malaria. *Trans R Soc Trop Med Hyg* 85(3):362–364.
7. Newton CR, et al. (1994) Brain swelling and ischaemia in Kenyans with cerebral malaria. *Arch Dis Child* 70(4):281–287.
8. Potchen MJ, et al. (2012) Acute brain MRI findings in 120 malawian children with cerebral malaria: new insights into an ancient disease. *AJNR Am J Neuroradiol* 33(9): 1740–1746.
9. Newton CR, et al. (1997) Intracranial hypertension in Africans with cerebral malaria. *Arch Dis Child* 76(3):219–226.
10. Walker O, et al. (1992) Prognostic risk factors and post mortem findings in cerebral malaria in children. *Trans R Soc Trop Med Hyg* 86(5):491–493.
11. SenGupta SK, Naraqi S (1992) The brain in cerebral malaria: A pathological study of 24 fatal cases in Papua New Guinea. *P N G Med J* 35(4):270–274.
12. Rest JR (1982) Cerebral malaria in inbred mice. I. A new model and its pathology. *Trans R Soc Trop Med Hyg* 76(3):410–415.
13. White NJ, Turner GDH, Medana IM, Dondorp AM, Day NPJ (2010) The murine cerebral malaria phenomenon. *Trends Parasitol* 26(1):11–15.
14. Hunt NH, Grau GE (2003) Cytokines: accelerators and brakes in the pathogenesis of cerebral malaria. *Trends Immunol* 24(9):491–499.
15. Rénia L, Grüner AC, Snounou G (2010) Cerebral malaria: In praise of epistemes. *Trends Parasitol* 26(6):275–277.
16. Riley EM, et al. (2010) Neuropathogenesis of human and murine malaria. *Trends Parasitol* 26(6):277–278.
17. Medana IM, Turner GD (2006) Human cerebral malaria and the blood-brain barrier. *Int J Parasitol* 36(5):555–568.
18. Polder TW, Eling WM, Curfs JH, Jerusalem CR, Wijers-Rouw M (1992) Ultrastructural changes in the blood-brain barrier of mice infected with Plasmodium berghei. *Acta Leiden* 60(2):31–46.
19. Penet MF, et al. (2005) Imaging experimental cerebral malaria in vivo: signiflcant role of ischemic brain edema. *J Neurosci* 25(32):7352–7358.
20. Zelenina M (2010) Regulation of brain aquaporins. *Neurochem Int* 57(4):468–488.
21. Nielsen S, et al. (1997) Specialized membrane domains for water transport in glial cells: High-resolution immunogold cytochemistry of aquaporin-4 in rat brain. *J Neurosci* 17(1):171–180.
22. Verkman AS, Ratelade J, Rossi A, Zhang H, Tradtrantip L (2011) Aquaporin-4: Orthogonal array assembly, CNS functions, and role in neuromyelitis optica. *Acta Pharmacol Sin* 32(6):702–710.
23. Medana IM, et al. (2011) Coma in fatal adult human malaria is not caused by cerebral oedema. *Malar J* 10:267.
24. Ampawong S, et al. (2011) Quantitation of brain edema and localisation of aquaporin 4 expression in relation to susceptibility to experimental cerebral malaria. *Int J Clin Exp Pathol* 4(6):566–574.
25. Grau GE, et al. (1991) Late administration of monoclonal antibody to leukocyte function-antigen 1 abrogates incipient murine cerebral malaria. *Eur J Immunol* 21(9): 2265–2267.
26. Wiese L, Kurtzhals JA, Penkowa M (2006) Neuronal apoptosis, metallothionein expression and proinflammatory responses during cerebral malaria in mice. *Exp Neurol* 200(1):216–226.
27. Waknine-Grinberg JH, et al. (2010) Artemisone effective against murine cerebral malaria. *Malar J* 9:22.
28. Preston GM, Carroll TP, Guggino WB, Agre P (1992) Appearance of water channels in Xenopus oocytes expressing red cell CHIP28 protein. *Science* 256(5055):385–387.
29. Agre P, et al. (2002) Aquaporin water channels—from atomic structure to clinical medicine. *J Physiol* 542(pt 1):3–16.
30. Hasegawa H, Ma TH, Skach W, Matthay MA, Verkman AS (1994) Molecular cloning of a mercurial-insensitive water channel expressed in selected water-transporting tissues. *J Biol Chem* 269(8):5497–5500.
31. Jung JS, et al. (1994) Molecular characterization of an aquaporin cDNA from brain: Candidate osmoreceptor and regulator of water balance. *Proc Natl Acad Sci USA* 91(26):13052–13056.
32. Lu MQ, et al. (1996) The human AQP4 gene: definition of the locus encoding two water channel polypeptides in brain. *Proc Natl Acad Sci USA* 93(20):10908–10912.
33. Neely JD, Christensen BM, Nielsen S, Agre P (1999) Heterotetrameric composition of aquaporin-4 water channels. *Biochemistry* 38(34):11156–11163.
34. Furman CS, et al. (2003) Aquaporin-4 square array assembly: Opposing actions of M1 and M23 isoforms. *Proc Natl Acad Sci USA* 100(23):13609–13614.
35. Gunnarson E, Zelenina M, Aperia A (2004) Regulation of brain aquaporins. *Neuroscience* 129(4):947–955.
36. Nagelhus EA, et al. (1998) Aquaporin-4 water channel protein in the rat retina and optic nerve: Polarized expression in Müller cells and fibrous astrocytes. *J Neurosci* 18(7):2506–2519.
37. Neely JD, et al. (2001) Syntrophin-dependent expression and localization of Aquaporin-4 water channel protein. *Proc Natl Acad Sci USA* 98(24):14108–14113.
38. Binder DK, Nagelhus EA, Ottersen OP (2012) Aquaporin-4 and epilepsy. *Glia* 60(8): 1203–1214.
39. Manley GT, et al. (2000) Aquaporin-4 deletion in mice reduces brain edema after acute water intoxication and ischemic stroke. *Nat Med* 6(2):159–163.
40. Amiry-Moghaddam M, et al. (2003) An alpha-syntrophin-dependent pool of AQP4 in astroglial end-feet confers bidirectional water flow between blood and brain. *Proc Natl Acad Sci USA* 100(4):2106–2111.
41. Papadopoulos MC, Manley GT, Krishna S, Verkman AS (2004) Aquaporin-4 facilitates reabsorption of excess fluid in vasogenic brain edema. *FASEB J* 18(11):1291–1293.
42. Tait MJ, Saadoun S, Bell BA, Verkman AS, Papadopoulos MC (2010) Increased brain edema in aqp4-null mice in an experimental model of subarachnoid hemorrhage. *Neuroscience* 167(1):60–67.
43. Amiry-Moghaddam M, et al. (2003) Delayed K+ clearance associated with aquaporin-4 mislocalization: phenotypic defects in brains of alpha-syntrophin-null mice. *Proc Natl Acad Sci USA* 100(23):13615–13620.
44. Binder DK, et al. (2006) Increased seizure duration and slowed potassium kinetics in mice lacking aquaporin-4 water channels. *Glia* 53(6):631–636.
45. Eid T, et al. (2005) Loss of perivascular aquaporin 4 may underlie deficient water and K+ homeostasis in the human epileptogenic hippocampus. *Proc Natl Acad Sci USA* 102(4):1193–1198.
46. Saadoun S, et al. (2005) Involvement of aquaporin-4 in astroglial cell migration and glial scar formation. *J Cell Sci* 118(Pt 24):5691–5698.
47. Ransohoff RM (2012) Illuminating neuromyelitis optica pathogenesis. *Proc Natl Acad Sci USA* 109(4):1001–1002.
48. McKeon A, et al. (2008) CNS aquaporin-4 autoimmunity in children. *Neurology* 71(2): 93–100.
49. Lennon VA, et al. (2004) A serum autoantibody marker of neuromyelitis optica: Distinction from multiple sclerosis. *Lancet* 364(9451):2106–2112.
50. Lennon VA, Kryzer TJ, Pittock SJ, Verkman AS, Hinson SR (2005) IgG marker of optic-spinal multiple sclerosis binds to the aquaporin-4 water channel. *J Exp Med* 202(4): 473–477.
51. Hinson SR, et al. (2012) Molecular outcomes of neuromyelitis optica (NMO)-IgG binding to aquaporin-4 in astrocytes. *Proc Natl Acad Sci USA* 109(4):1245–1250.
52. Madrid R, et al. (2001) Polarized trafficking and surface expression of the AQP4 water channel are coordinated by serial and regulated interactions with different clathrin-adaptor complexes. *EMBO J* 20(24):7008–7021.
53. Yamamoto N, et al. (2001) Alterations in the expression of the AQP family in cultured rat astrocytes during hypoxia and reoxygenation. *Brain Res Mol Brain Res* 90(1):26–38.
54. Fu X, Li Q, Feng Z, Mu D (2007) The roles of aquaporin-4 in brain edema following neonatal hypoxia ischemia and reoxygenation in a cultured rat astrocyte model. *Glia* 55(9):935–941.
55. Lee M, et al. (2008) Regulation of AQP4 protein expression in rat brain astrocytes: Role of P2X7 receptor activation. *Brain Res* 1195:1–11.
56. Meng S, et al. (2004) Correspondence of AQP4 expression and hypoxic-ischaemic brain oedema monitored by magnetic resonance imaging in the immature and juvenile rat. *Eur J Neurosci* 19(8):2261–2269.
57. Machado FS, et al. (2006) Endothelin in a murine model of cerebral malaria. *Exp Biol Med (Maywood)* 231(6):1176–1181.
58. Koyama Y, Tanaka K (2010) Decreases in rat brain aquaporin-4 expression following intracerebroventricular administration of an endothelin ET B receptor agonist. *Neurosci Lett* 469(3):343–347.
59. Mohanty D, et al. (1997) Fibrinolysis, inhibitors of blood coagulation, and monocyte derived coagulant activity in acute malaria. *Am J Hematol* 54(1):23–29.
60. Tang YP, Cai DF, Chen YP (2007) Thrombin inhibits aquaporin 4 expression through protein kinase C-dependent pathway in cultured astrocytes. *J Mol Neurosci* 31(1): 83–93.
61. Hemmer CJ, et al. (1991) Activation of the host response in human Plasmodium falciparum malaria: Relation of parasitemia to tumor necrosis factor/cachectin, thrombin-antithrombin III, and protein C levels. *Am J Med* 91(1):37–44.
62. Thrane AS, et al. (2011) Critical role of aquaporin-4 (AQP4) in astrocytic Ca2+ signaling events elicited by cerebral edema. *Proc Natl Acad Sci USA* 108(2):846–851.
63. Vajda Z, et al. (2000) Increased aquaporin-4 immunoreactivity in rat brain in response to systemic hyponatremia. *Biochem Biophys Res Commun* 270(2):495–503.
64. Yuan JS, Reed A, Chen F, Stewart CN (2006) Statistical analysis of real-time PCR data. *BMC Bioinformatics* 7:7.